CHEMICAL PROBLEMS OF THE DEVELOPMENT OF NEW MATERIALS AND TECHNOLOGIES
Minsk 2003

G. A. Ragoisha,
A. S. Bondarenko

POTENTIODYNAMIC ELECTROCHEMICAL IMPEDANCE SPECTROSCOPY

INTRODUCTION

Electrochemical response of the electrochemical interface contains valuable information on charge transfer, adsorption, desorption, surface reactions and the space charge and diffusion layers in the electrode and solution. A great number of techniques has been developed to acquire and analyse electrochemical response and its time-frequency-potential variance [1–3]. Exploration of the time-frequency-potential relationship of an electrochemical system with common techniques is lengthy and laborious, moreover the successive application of several techniques for versatile characterisation of short-lived states is generally impossible. However, with the progress of digital techniques the integration of different probing procedures in a single electrochemical experiment becomes increasingly possible [4–8].

Personal computers have been long used in electrochemical laboratories, but ordinary computerisation just automated the common electrochemical equipment. With increasing power of computers and programming facilities a new generation of the electrochemical digital techniques evolve. The new digital instrumentation explores the transfer functions evolution in both potential and time with extensive usage of virtual instruments that impart more power and flexibility to the probing procedures and analysis of the response. Transfer function analysis has proved to be efficient in many fields of science and engineering [9], however the usage of digital signal processing in electrochemistry is not thus straightforward as in electronic or optical applications. The problems originate from nonlinearity and non-stationarity of most electrochemical systems. The electrochemical responses may often be assumed to be linear functions of driving force in ac experiments involving single frequencies and small amplitudes, e.g. in conventional electrochemical impedance spectroscopy that takes the transfer function snapshots at certain well-defined states of the system (usually stationary, constant potential states). The situation becomes more complex with the superposition of many frequencies in non-stationary systems.

One method that has been widely advocated is the Fourier analysis of time-varying systems [4, 5, 10, 11]. However, despite its ability to probe ac and dc properties rapidly and near-simultaneously, this approach has not replaced much slower and independent ac and dc voltammetry. In our opinion the main reason for this is the lack of additivity of multi-frequency electrochemical signals used in Fourier transform techniques. There are several reasons for signal degradation in

the multi-frequency probing. First, the responses in different frequencies may differ in orders of magnitude, so the conditions for the detection and analysis are also different for various signal components. Small non-linear perturbations of powerful components, unimportant in the single-frequency probing, may jam low-level components in the multi-frequency signal. Second, the possible electrochemical system non-stationarity and multi-stability in the potential scan, that will be discussed later, introduces the possibility of inter-frequency interactions.

The investigation of the electrode surface by the electrochemical probing in its complexity resembles the observation of the Earth surface from satellite through dusty atmosphere. In both cases the counters of the object under investigation are not observable directly and strenuous effort is required to recognise them in the response.

The development of digital electrochemical techniques in Belarusian State University was reviewed by 2001 in [6]. In this review we shall consider the latest developments in the potentiodynamic electrochemical impedance spectroscopy (PDEIS) – the new digital technique that provides simultaneous ac and dc probing of electrochemical systems and the analysis of the responses just in the potential scan.

PDEIS uses wavelets in the time domain, rather than multi-frequency analysis in the frequency domain, to explore the time-frequency-potential relationship of an electrochemical system [6–8, 12]. This helps to minimise inter-process perturbations in systems exhibiting non-stationarity and insures low-level detection in presence of noise. Moreover, the response analysis is implemented in PDEIS along the trajectory of the potential scan, so in a simple experiment the investigator gets the potentiodynamic voltammogram, plus the Nyquist and Bode plots extended to 3D as a function of potential. Individual Nyquist and Bode plots may therefore readily be extracted from the 3D plots as orthogonal sections and decomposed by a built-in equivalent circuit analyser into the constituent responses of the circuit elements, analogous to conventional ac impedance measurements [7]. This is especially useful in the investigation of short-lived states.

The basics of PDEIS have been described in [7]. We shall not replicate here the information from [7], as its electronic version is posted on Chemweb.

First some data on PDEIS application to stationary reversible systems will be considered on the example of $[Fe(CN)_6]^{3-}/[Fe(CN)_6]^{4-}$ redox system analysis. Then we will proceed with non-stationary systems, using underpotential metal monolayers deposition for the illustration and, finally, show how PDEIS can be applied in the investigation of more complex nanophases on the example of a hydrated nickel oxide ultra-thin film on nickel.

1. PDEIS OF STATIONARY SYSTEMS

Though the main destination of PDEIS is rapid exploration of non-stationary electrochemical systems, its application in stationary system analysis is also advantageous.

The usual sequence of operations in PDEIS investigation of an electrochemical system comprises automated probing of ac and dc responses in the potential scan in the experiment similar to the acquisition of a potentiodynamic voltammogram,

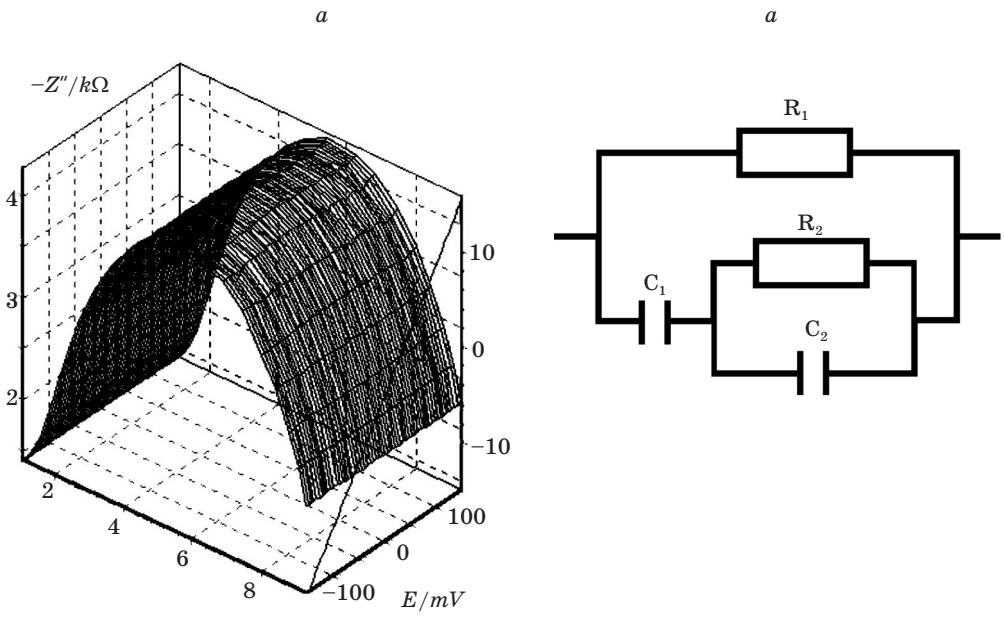

Fig. 1. (*a*) PDEIS spectrum of a sample circuit (*b*);
R_1= 10 kΩ, R_2= 1.8 kΩ, C_1 = 0.12 μF, C_2 = 0.25μF

the fitting of the PDEIS spectrum to equivalent electric circuits (EEC) with the analyser built into the program of the virtual spectrometer and, finally, the analysis of the EEC parameters on the potential scale.

We'll begin the demonstration of PDEIS operation from the simplest object - a dummy cell composed of several active and reactive elements. This is just to show the adequacy of the physical quantities obtained at the output.

Fig. 1 shows the PDEIS spectrum of a sample circuit. The parameters obtained (R – resistance, C – capacitance) conform to the actual circuit used in this test. Running a spectrometer program on template circuits is a simple and fast operation test for the probing and analysis routines.

Unlike the capacitors and resistors that do not vary with the potential, the electrochemical system parameters are the functions of the potential. For the stationary systems the theory is well developed [13], so the analysis of the PDEIS spectra of stationary systems on the potential scale provides easy determination of physical quantities involved in the equations of the electrochemical kinetics, e.g. diffusion coefficient D can be calculated from Warburg constant dependence on potential E:

$$\sigma(E) \quad \frac{4RT}{n^2F^2A\sqrt{2Dc_i}}\cosh^2 \quad \frac{nF}{2RT}(E \quad E_{1/2}) \qquad (1)$$

where A – surface area, c_i – bulk concentration of the electroactive component i in the solution, the other symbols have their usual meaning.

Similarly, using the same equation, an electrode surface A can be accurately determined from the spectrum of a known system.

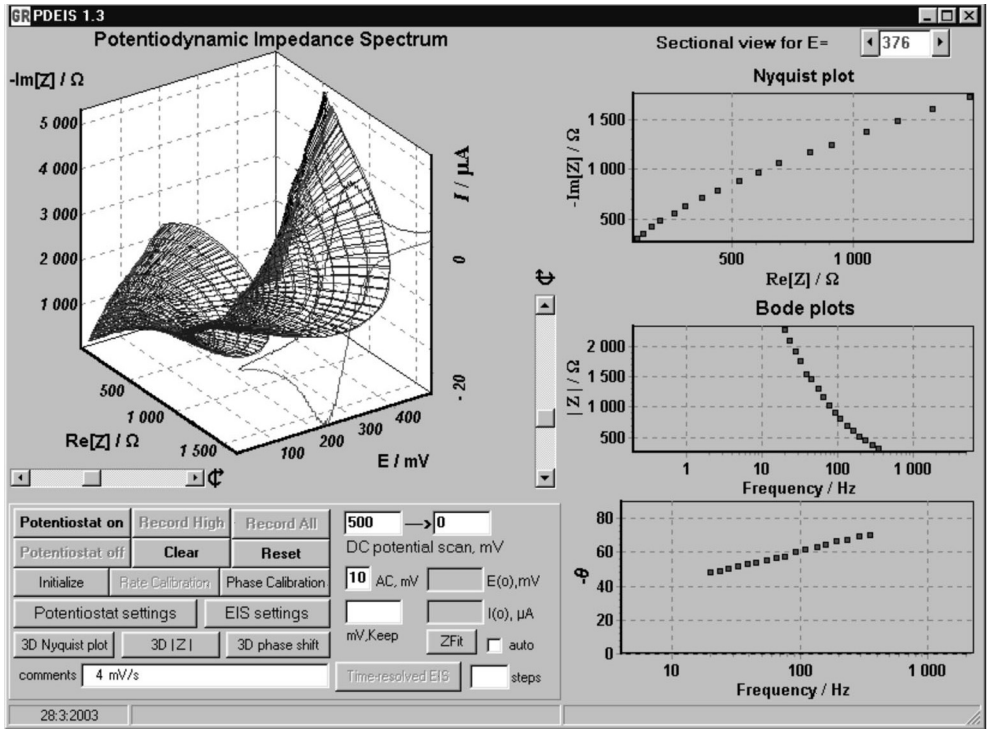

Fig. 2. The view of the PDEIS spectrometer screen in cyclic potential scanning of glassy carbon electrode in 5.2 mM $K_3[Fe(CN)_6]$ + 1M KCl

Fig. 2 shows a view of the PDEIS spectrometer screen in the first stage of $[Fe(CN)_6]^{3-}/[Fe(CN)_6]^{4-}$ system analysis. Though a tremendous number of measurements and computation is involved in this simple experiment, all the work is done in the background by a computer. For the investigator a PDEIS spectrum acquisition is no more complex than recording a cyclic voltammogram.

Three graphs on the right in Fig. 2 are the constant potential sections of the PDEIS spectrum, shown in the form of Nyquist and Bode plots. The information in these graphs is dynamically renewed during the potential scan. The 3D spectrum on the left accumulates the information on impedance spectra dependence on the potential. The 3D spectrum can be viewed from different perspectives in three coordinate systems corresponding to the Nyquist and Bode plots coordinates with the additional variable E – electrode potential (in all examples in this paper E was measured vs $Ag|AgCl|KCl_{sat}$). PDEIS spectrum is a portrait of the electrochemical system ac and dc response. It represents the transfer function in a limited range of frequencies.

The frequency range used in the impedance analysis needs some clarification. Conventional impedance spectroscopy of stationary states works over a wide rage of frequencies from a millihertz to a megahertz. Impedance analysis in the wide frequency range is intended to insure that none of the EEC elements is lost. However, the potentiostatic impedance spectra are often ambiguous even in the wide range of frequencies. To minimise the ambiguity Kramers-Kronig analysis is usually applied to check the consistency of impedance data [14–19].

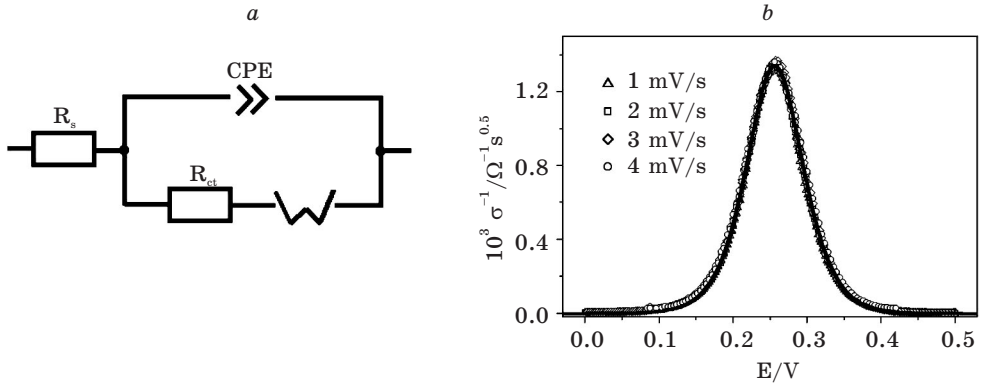

Fig. 3. (*a*) EEC deduced from the data represented by Fig. 2, (*b*) experimental inverse Warburg constant dependences on potential at different scan rates (open symbols) and calculated curve (solid line)

PDEIS treats this problem from a different perspective. The goal of the EEC analysis in PDEIS is the decomposition of the response into the constituents related with different processes represented by different elements in EEC. To achieve this goal, even a fraction of the impedance spectrum is sufficient, provided it contains the responses of the elements in question. The ambiguities of conventional equivalent circuits, deduced at single potentials, are substantially removed by PDEIS, as the potential dependence of the circuit parameters gives additional physical insight that in turn restricts the choice of equivalent circuits over several hundred mV. The additional variable provides a more efficient removal of EEC ambiguity than a simple extension of the frequency range. The analysis from fifteen to thirty frequencies, depending on the complexity of the EEC, usually appears to be sufficient to decompose the response into constituents related to different EEC elements.

Fig.3a shows the EEC deduced from the data represented by Fig. 2. This circuit is a variant of Randles EEC with the double layer capacitance represented by a constant phase element (CPE). The impedance of CPE Z_{cpe} is very similar to the impedance of the capacitor in complex impedance notation:

$$Z_{cpe}=Q^{-1}(j\omega)^{-n} \qquad (2)$$

The exponent n in (2) is fractional and for the circuit shown in Fig. 3a is usually close to 1, so the parameter Q is treated as a pseudocapacitance that behaves similar to the capacitance but gives a phase shift slightly less than $\pi/2$ radians.

The branch of the EEC connected in parallel with CPE is the Faraday impedance. In this example it consists of a charge transfer resistance R_{ct} and Warburg impedance Z_w (impedance of the diffusion), the latter has the following frequency dependence in complex impedance notation:

$$Z_w= \sigma/(j\omega)^{0.5} \qquad (3)$$

where σ is the Warburg constant that has been already represented by its dependence on the potential in the equation (1).

Fig. 3b shows the plots of experimental σ(E) data in cyclic scans at different scan rates for glassy carbon electrode in 5.2 mM $K_3[Fe(CN)_6]$ + 1M KCl and the corresponding calculated curve. The independence of the data on the scan rate and their fit to the theory both in the catodic and anodic scan result from the reversibility of $K_3[Fe(CN)_6]/K_4[Fe(CN)_6]$ system.

3. UPD INVESTIGATION WITH PDEIS

A quite different case is represented by the electrochemical formation of surface adsorption structures and monolayers deposited by cathodic reduction of metal ions above Nernst potential (the letter process is called underpotential deposition, or UPD [20, 21]). The importance of PDEIS for this kind of objects can be illustrated by the analogy on the comparison of potentiodynamic and potentiostatic voltammetry. Suppose, one investigates UPD with cyclic voltammetry and gradually decreases the scan rate approximating the stationary case. (S)he would get informative cathodic and anodic peaks at moderate scan rates but at very low scan rates the voltammogram degenerates into a trivial zero line that gives no information on the UPD. The same is with the potentiodynamic and potentiostatic impedance measurements. The potentiostatic impedance measurement can detect the monolayer, formed as the result of UPD, but cannot characterise the UPD itself with its intrinsic complexity.

We shall present several examples to illustrate this new physical insight on the surface reactions provided by PDEIS. Let us first consider copper monolayer formation on polycrystalline gold, omitting the experimental details described in [8].

Fig. 4 shows PDEIS spectra of Cu UPD on Au (Figs 4a and 4b), along with cyclic voltammograms (Fig. 4c), and Fig. 5 – the EEC deduced from the spectra shown in Fig. 4 and similar spectra with sulphate substituted by nitrate in the solution (Fig. 5a), with the dependences of the EEC parameters on the potential in the cyclic potential scan (Figs 5b–5f).

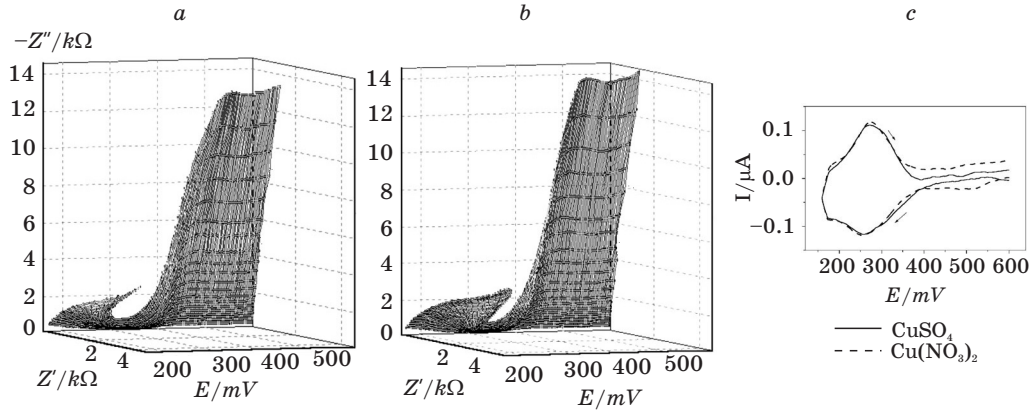

Fig. 4. Cu UPD on Au. (*a*, *b*) PDEIS spectra:
(*a*) cathodic (*b*) anodic branch of the cyclic potential scan in 0.1M H_2SO_4 + 10 mM $CuSO_4$;
(*c*) cyclic voltammograms of Au in 0.1M H_2SO_4 + 10 mM $CuSO_4$
and 0.1M HNO_3 + 10 mM $Cu(NO_3)_2$. dE/dt = 2 mV/s

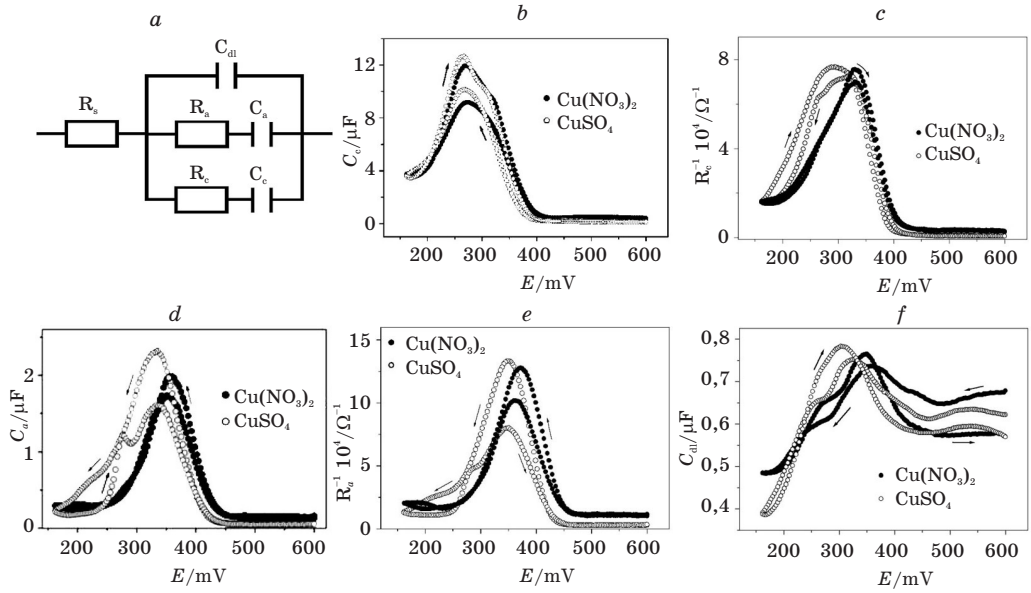

Fig. 5. Cu UPD on Au. (*a*) Equivalent electric circuit; (*b–f*) the dependencies of the equivalent circuit parameters on potential corresponding to the voltammogram in Fig. 4*c*

Unlike the PDEIS spectra, discussed in the previous section, the PDEIS spectra in the latter case disclose the differences in the electrode state in the cathodic and anodic scans, showing intrinsic irreversibility and non-stationarity of the underlying processes and also the differences in the behaviour of different anions in the UPD. Anion effects in Cu UPD on Au have been observed in earlier investigations [20], but stationary techniques fail to characterise the dynamics of anion co-adsorption in UPD and, also, the potentiodynamic voltammetry gives only a small part of the electrochemical response and misses completely the differences in Cu UPD with different anions (Fig. 4c).

The branch of the circuit with the elements labelled with subscript *c* may be ascribed to Cu UPD, as the capacitance C_c is the highest of the three capacitances in Fig. 5a and shows the closest correlation with the voltammogram. By contrast, the capacitance C_a shows just a small peak at the current maximum on the reverse scan in sulphate, and the main C_a peaks are shifted to more positive potentials. The C_c peak is lower on the cathodic scan than on the anodic scan, while the C_a peak, by contrast, is lower on the anodic scan. The inverse of R_a correlates well with C_a, and both show a positive shift in nitrate. The double layer capacitance reveals the effect of the anions and shows how this can vary with potential.

The equivalent circuit branch having elements marked with the subscript *a* belongs to the anion adsorption that is known to accompany Cu upd on Au [20]. Fig. 5 tells us much about the anion effect. First, comparison of the data from Figs 5d and 5e with the voltammograms in Fig. 4c makes clear that the coordination of the anions by the adatoms starts in the cathodic scan at approx. 450 mV, long before the rise in the cathodic current. Second, the effect of nitrate fades out before the UPD current maximum, while the sulphate effect persists much longer. Third, the reverse scan in the sulphate solution shows two anion desorption pro-

cesses. The first one is near the current maximum and the second one is in the final stage of the monolayer anodic oxidation process.

The significant increase in the C_c capacitance and its complex dependence on the potential on the reverse (anodic) scan uncover the intrinsic irreversibility of the process. Surprisingly, the discharge of the capacitance C_c on the anodic scan requires more charge than that injected on the cathodic scan (Fig. 5b). A clue to this puzzle lies in the charging and discharging of the anion adsorption pseudocapacitance C_a (Fig. 5d). Evidently the forward and backward charge transfer processes take place on different structures formed by Cu atoms with the surroundings. Unfortunately, the nature of these structures is unclear [20] and further work is required to elucidate them.

As an illustration of the possibilities for the quantitative analysis of the constituent responses provided by PDEIS, Fig. 6 shows the cathodic curves from Fig. 5d together with the simulated curves obtained assuming a Langmuir adsorption isotherm for anions. The model also assumes one-electron transfer with a transfer coefficient of 0.5. With these assumptions, the dependences of the adsorption pseudocapacitance and pseudoresistance on the potential can be represented as [22]:

$$C_a = Fq_a/4RT\cosh^2(0.5F\eta/RT) \quad (4)$$

$$R_a^{\ 1} = F^2k_0/2RT\cosh(0.5F\eta/RT) \quad (5)$$

where q_a is the charge of the maximum surface coverage by the adsorbate, η is the overpotential, and k_0 is the standard rate constant. The other symbols have their usual meaning. According to the equations (4-5) C_a and R_a^{-1} are both the functions of overpotential with maxima at $\eta = 0$. In the early stages of nitrate and sulphate adsorption the $C_a(E)$ plots fit this model quite well (Fig. 6), thus revealing that adsorption is initially reversible. However, below 0.3 V the experimental values diverge considerably from the model thus disclosing a more complex character of anion adsorption in the next stage of the monolayer growth.

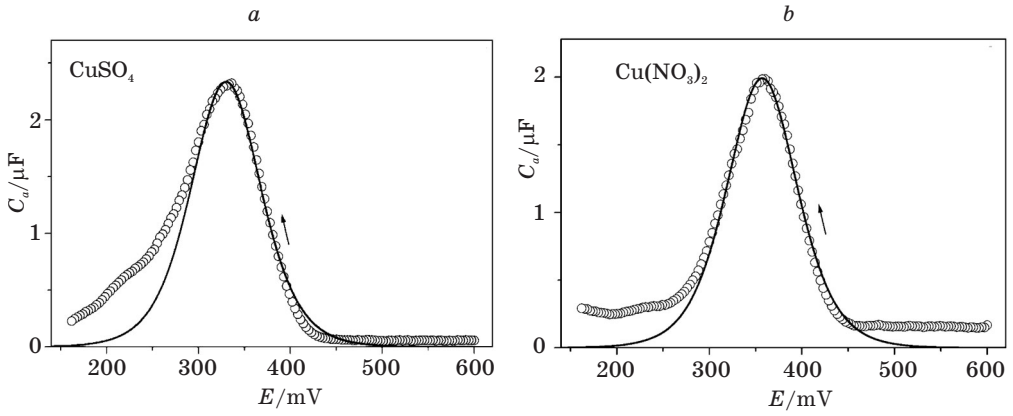

Fig. 6. The simulated dependences of anion adsorption pseudocapacitance on potential in the cathodic scan (solid lines) with the data from Fig. 5*d* (circles); (*a*) sulphate electrolyte, (*b*) nitrate electrolyte

Fig. 7 shows one more example of UPD on Au [23]. In this case (Te UPD on Au) the irreversibility of the underlying processes is obvious even from the voltammogram that gives more than 250 mV difference for the cathodic and anodic peaks. The potentiodynamic impedance analysis discloses a considerable hysteresis in the cyclic variation of the double layer pseudocapacitance (Fig. 7e). The monolayer deposition decreases the initially high double layer capacitance of Au surface, while the subsequent stripping of the monolayer in the anodic scan increases the capacitance. Again, interesting features unobservable with cyclic voltammetry emerge from the impedance analysis on the potential scale. In the anodic scan in the potential range below the monolayer oxidation potential the double layer capacitance increases gradually, due to reorganisation in the double electric layer formed on Te monolayer but in the very beginning of the monolayer anodic oxidation the adsorption structures that prevented the monolayer from destruction collapse resulting in a decrease in the capacitance just before its rise in the anodic reaction.

Fig. 8 shows a somewhat different behaviour of the double layer capacitance in Bi UPD on Pt [23]. Bismuth ions adsorb strongly on platinum, so the whole $Q(E)$ curve is lifted considerably compared to $Q(E)$ for the bare platinum surface in nitric acid. A series of transformations in the double layer in the UPD range is

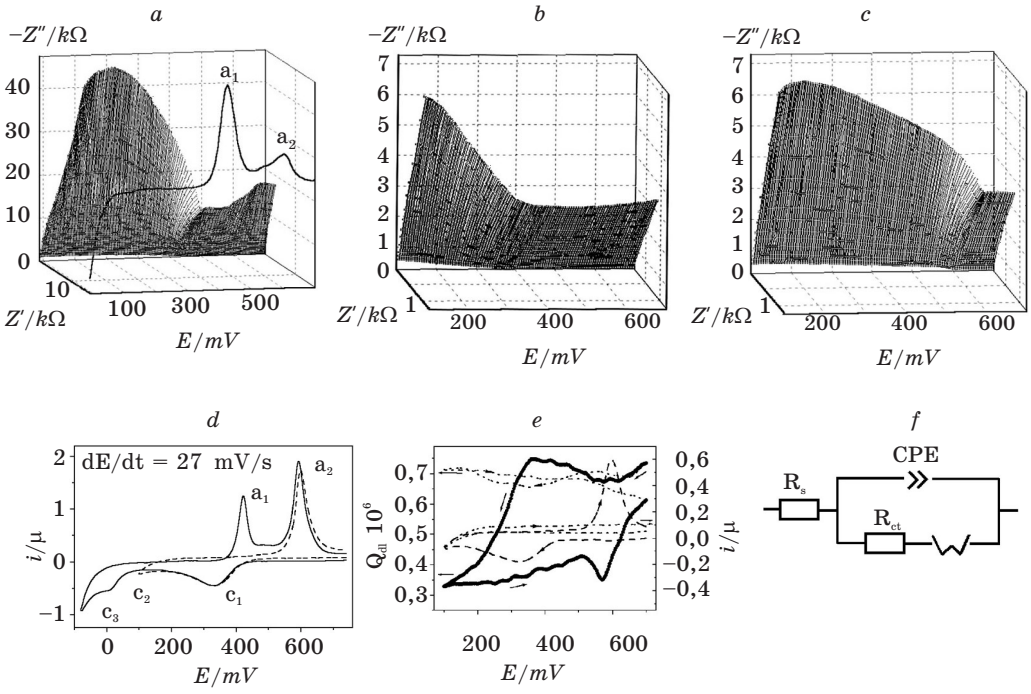

Fig. 7. Tellurium upd on Au in 0.1M H_2SO_4+2mM TeO_2. (a) PDEIS spectrum and the voltammogram for combined Te nanoparticles (a_1) and monolayer (a_2) oxidation in the anodic scan; (*b*, *c*) PDEIS spectra of Te monolayer, (*b*) cathodic, (*c*) anodic scan; (*d*) cyclic voltammograms with different reversal potentials; (*e*) Q_{dl} dependence on potential (solid circles) and cyclic voltammogram (dashed). Dotted lines show the reference dependencies in absence of Te. (f) EEC. dE/dt = 7.6 mV/s except for (*d*)

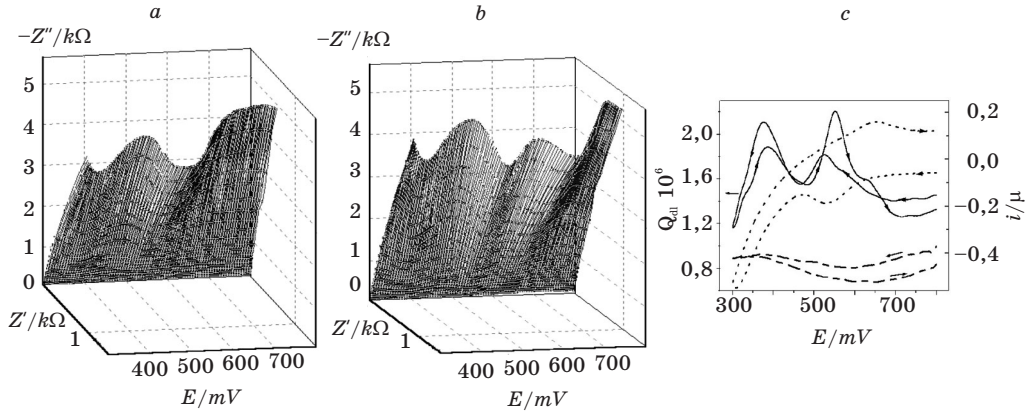

Fig. 8. Bi upd on Pt in 0.3M HNO_3+5mM $Bi(NO_3)_3$.
(*a*, *b*) PDEIS spectra, (*a*) cathodic, (*b*) anodic scan; (*c*) Q_{dl} dependence
on potential (solid) with the corresponding cyclic voltammogram (dotted).
The dashed line shows the reference Q_{dl} in absence of bismuth.
The EEC is the same as in Fig. 7*f*. dE/dt =2.6 mV/s

disclosed by the potentiodynamic impedance analysis and, again, the cyclic voltammetry overlooks these changes.

Fig. 9a illustrates the other kind of cyclic changes in the double layer capacitance by Pb UPD on tellurium. The latter system has been investigated in collaboration with E.A.Streltsov and N.P.Osipovich [24,25].

The original double layer capacitance on tellurium surface is much lower than the capacitance of a new double electric layer emerging during Pb monolayer deposition. So various effects in the UPD could be easily observed through the changes of the double layer capacitance. Fig.9a shows the effect of halides (chloride,

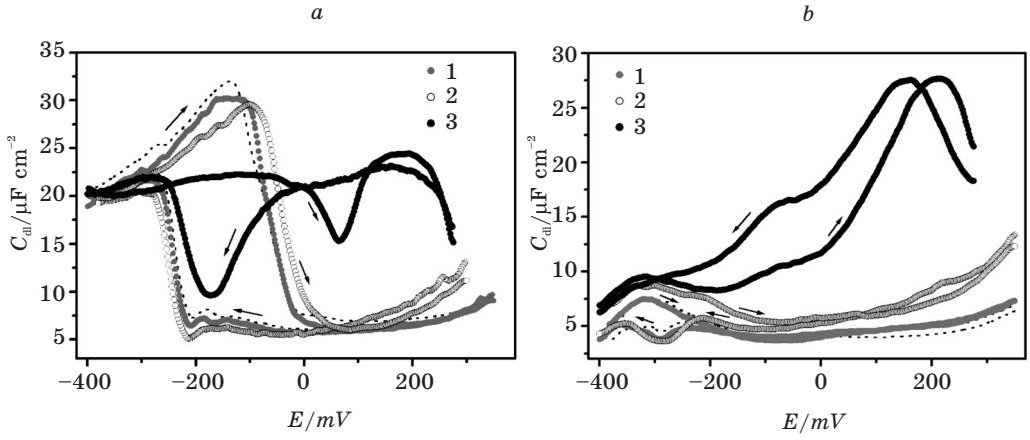

Fig. 9. Tellurium electrode C_{dl} dependences on potential
in (a) 1mM $Pb(NO_3)_2$+0.1M HNO_3+1.5 mM KHal
and (b) in 0.1M HNO_3+1.5 mM KHal (1 – KCl, 2 – KBr, 3 – KI).
Dotted lines show the reference dependences in absence of halide.
dE/dt=2.35 mV/s , scan directions are shown with arrows

bromide and iodide) and Fig. 9b gives for the reference Te double layer capacitance dependence on the potential in absence of lead with the same halides. A strong effect of iodide was observed both for the double layer on Te surface and on Pb monolayer with a lot of additional fine effects that were beyond the scope of the potentiodynamic voltammetry and impedance spectroscopy of stationary states. We would like to note that in the case of Pb UPD on Te potentiostatic impedance measurements were unavailing because of Pb monolayer interaction with Te substrate in the time scale of common impedance spectroscopy. PDEIS resolved this problem by the potential cyclic scanning fast enough to prevent the monolayer from the subsequent spontaneous reaction.

3. NANOPHASES INVESTIGATION WITH PDEIS

Simultaneous monitoring and analysis of dc and ac responses with PDEIS are also helpful in the investigation of deeper chemical transformations on the interface following the adsorption effects and the monolayer formation. By considering the out-of-phase response component PDEIS gives a three-dimensional view to a common potentiodynamic voltammetry that detects just the in-phase response of the electrochemical system. Some examples are: a new phase growth monitoring by the increase in the double layer capacitance that results from the increase in electrode surface area, detection of the unusual catalytic activity of nanoparticles [7], monitoring of nanoparticles oxidation by the decrease in both the real and imaginary impedance components [7, 25].

The following example illustrates the PDEIS application for the monitoring of electrochemically stimulated changes in ultrathin oxide films.

Fig. 10a shows the best fit EEC for Ni electrode pretreated with concentrated HCl and cycled afterwards in 1.0 M NaOH between –200 mV and –900 mV, and Fig. 10b – the corresponding variation of the double layer pseudocapacitance Q_{dl} with the potential. Q_{dl} exhibits an increase on the reverse (anodic) scan for the electrode scanned below –700 mV. The effect of the cathodic treatment is presented in more detail in Fig. 11 that shows the variation with the potential of EEC

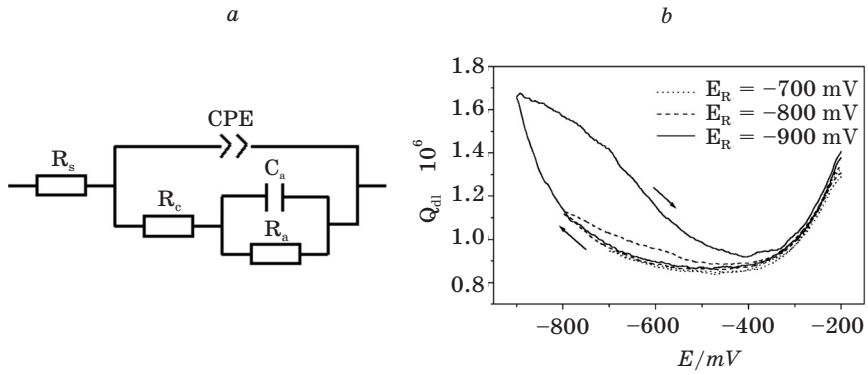

Fig. 10. Nickel electrode in 1M NaOH. (a) EEC and (b) double layer pseudocapacitance cyclic variation with the potential; dE/dt=0.6 mV/s

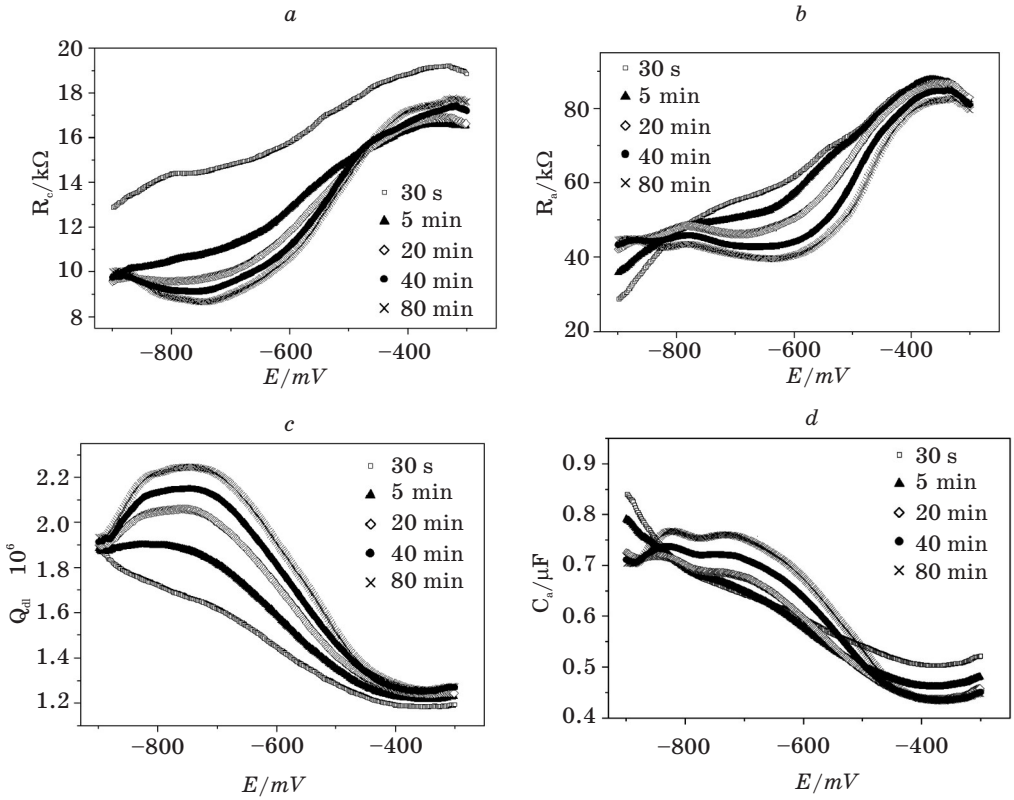

Fig. 11. Nickel electrode in 1M NaOH at different duration of pretreatment at -900 mV. Variation of EEC parameters in the anodic scan; dE/dt=0.6 mV/s

elements in the anodic scan at different holding time at -900 mV. With the increase in the time of a hydrated oxide film reduction the extrema in Q_{dl} and R_c develop at approx. –750 mV, while R_a attains the minimum at approx. –650 mV. The minima in R_c and R_a have been assigned to the formation of, correspondigly, α–$Ni(OH)_2$ and its subsequent dehydration to β–$Ni(OH)_2$ at a higher potential. The assignment of the effects to the transformations involving α–$Ni(OH)_2$ and β–$Ni(OH)_2$ conforms with the earlier [26, 27] reported effect of the potential on the stability of different hydroxide forms on nickel. In this example R_c behaves as charge transfer resistance and R_a – as the active component of the sequentially connected adsorption psedoresistance.

CONCLUSION

PDEIS appears to be a powerful, fast and easy to use tool for the investigation of a wide range of phenomena on the electrochemical interfaces, from adsorption and electrochemical reactions to the transformations in nanophases.

REFERENCES

1. Techniques of Electrochemistry, E. Yeager and A.J. Salkind, John Wiley & Sons, 1973.
2. *Cottis R. A., Llewellyn A. M.* Electrochemical Techniques, UMIST, 1996; http://www.cp.umist.ac.uk/lecturenotes/Echem/index_main.htm.
3. *Eklund J. C., Bond A. M., Alden J. A., Compton R. G.* Perspectives in modern voltammetry: Basic concepts and mechanistic analysis (Adv. Phys. Organic Chem. 1999. Vol. 32. P. 1–120.
4. *Schiewe J., Hazi J., Vicente-Beckett V. A., Bond A. M.* J. Electroanal Chem. 1998. Vol. 451, P. 129–138.
5. *Walters M. J., Garland J. E., Pettit C. M., Zimmerman D. S., Marr D. R., Roy D.* J. Electroanal. Chem. 2001. Vol. 499, P. 48-60.
6. *Ragoisha G. A. and Bondarenko A. S.* Selected Proceedings of Belarusian State University. 2001. Vol. 5. P. 139–154.
7. *Ragoisha G. A., Bondarenko A. S.* Solid State Chemistry V (Solid State Phenomena, Vol. 90–91), Trans Tech Publ. 2003. P. 103–108; electronic preprint is available on Chemweb: http://preprint.chemweb.com/physchem/0301002.
8. *Ragoisha G. A. and Bondarenko A. S.* Electrochem. Commun. 2003. Vol. 5. P. 392–395.
9. *Smith S. W.* The Scientist and Engineer's Guide to Digital Signal Processing, California Tech. Publ. 1997.
10. *Garland J. E.,. Assiongbon K. A, Pettit C. M., Emery S. B. Roy, D.* Electrochim. Acta. 2002, Vol. 47, P. 4113–4124.
11. *Rueda M., Navarro I., Prado C., Silva C.* J. Electrochem. Soc. 2001, 148(4) E139–E147.
12. *Ragoisha G. A. and Bondarenko A. S.* Physics, Chemistry and Application of Nanostructures (World Scientific, 2001), 308-312.
13. *Lasia A.* Electrochemical Impedance Spectroscopy and its Applications, http://alfa.chem.uw.edu.pl/LasiaLecture/EIS1.pdf.
14. *Macdonald R.* LEVM Manual, J. Ross Macdonald and Solartron Group Limited, 1999.
15. *MacDonald J. R.* Impedance spectroscopy, John Wiley & Sons, 1987.
16. *Dygas J. R., Breiter M. W.* Electrochimica Acta, 1999, 44, 4163–4174.
17. *Orazem M. E., Durbha M., Deslouis C., Takenouti H., Tribollet B.* Electrochim. Acta, 1999, 44, 4403–4412.
18. *Diard J. P., Le Canut J. M., Le Gorrec B., Montella C.* Electrochim. Acta, 1998, 43(16–17), 2485–2501.
19. *Bisquert J., Garcia-Belmonte G., Fabregat-Santiago F., Compte A.* Electrochem. Commun. 1999, 1, 429–435.
20. *Herrero E., Buller L. J., Abruna H. D.* Chem. Rev. 2001, 101, 1897–1930.
21. D. M. Kolb, M. Przasnyski, H.Gerischer, J. Electroanal. Chem., 1974, 54, 25–38.
22. *Lasia A.* Applications of Electrochemical Impedance Spectroscopy to Hydrogen Adsorption, Evolution and Absorption into Metals, http://alfa.chem.uw.edu.pl/LasiaLecture/EIS2.pdf.
23. *Ragoisha G. A. and Bondarenko A. S.* Physics, Chemistry and Application of Nanostructures (World Scientific, 2003). P. 373. Electronic preprint: http://preprint.chemweb.com/physchem/0301005.
24. *Ragoisha G. A., Bondarenko A. S., Osipovich N. P. and Streltsov E. A.* Proc. of the 2nd Russian Conf. on Surface Chemistry and Nanotechnology, Hilovo – St. Petersburg, Sept. 24–29, 2002, 176–178.
25. *Ragoisha G. A., Bondarenko A. S., Osipovich N. P., Streltsov E. A.* J. Electroanal. Chem. 2003, submitted.
26. *Seghiouer A., Chevalet I., Barhoun A., Lantelme F. J.* of Electroanal. Chem. 442 (1998) 113–123.
27. *D'Alkaine C. V., Santanna M. A.* J. of Electroanal. Chem. 457 (1998) 5-12.